Preliminary image reconstruction results of simulated single-pinhole SPECT data using STIR

STIR User's and Developer's Meeting

Matthew Strugari

December 3, 2020

DALHOUSIE UNIVERSITY

BIOTIC Imaging for Life

CUBRESA Molecular Imaging Solutions

nova scotia health authority

© Matthew Strugari 2020

Disclosures

Academic-industry research collaboration between BIOTIC and Cubresa, Inc.

Tomographic reconstruction software is widely available

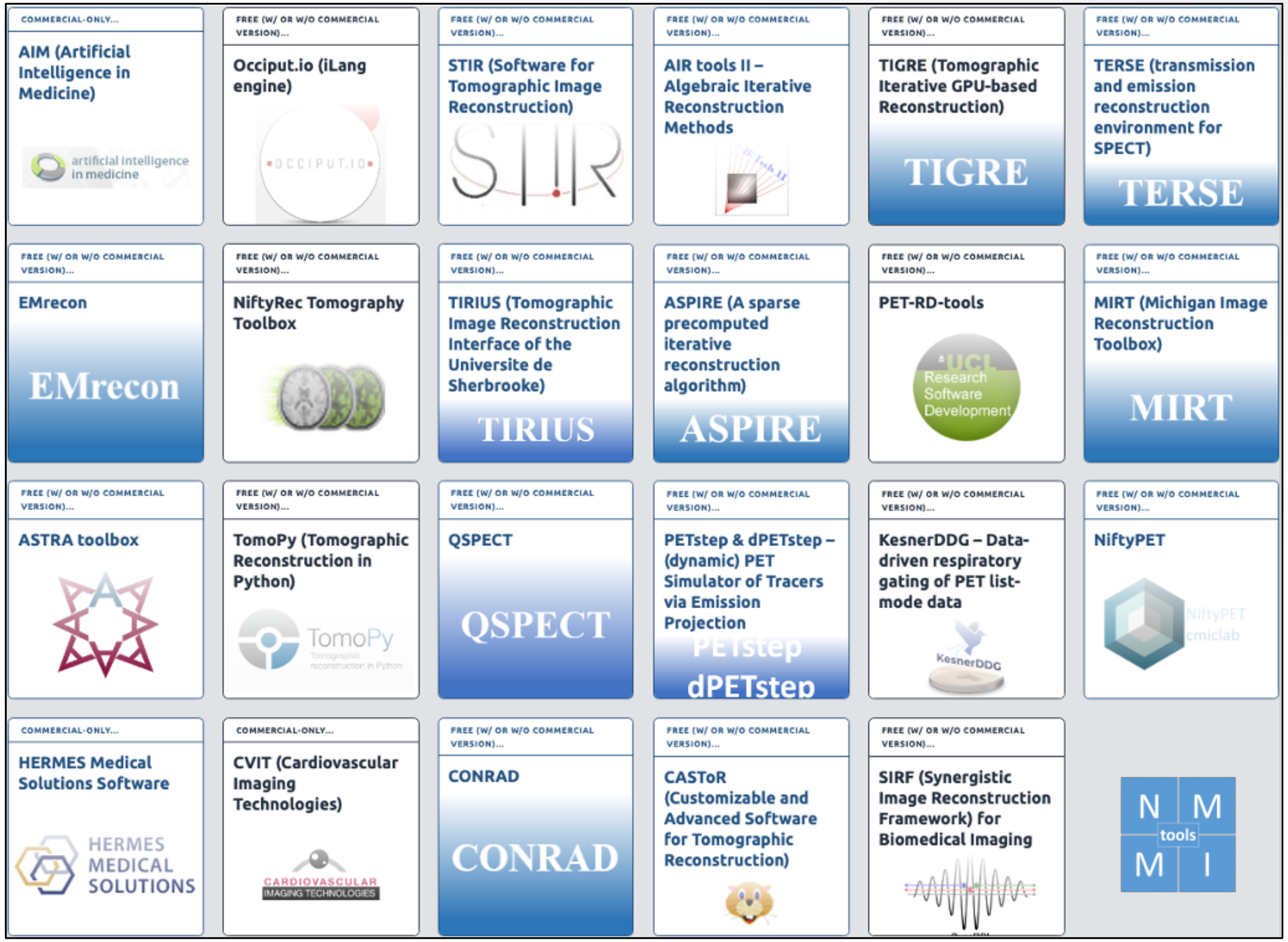

Figure 1. Tomographic image reconstruction software (NMItools)

- Open source and commercial software for PET, SPECT, and CT image reconstruction
  - Analytic and iterative 3D and 4D reconstruction algorithms
  - Mathematical, physical and physiological modelling
  - Data manipulation and presentation

What do they all have in common?

- No support for pinhole-SPECT

Prototype code has been developed to estimate the weight matrix in pinhole-SPECT

- Written for the **S**oftware for **T**omographic **I**mage **R**econstruction (**STIR**) by Carlés Falcón in 2014 (author of SPECT UB code for parallel and convergent collimators)

Weight matrix estimation for **single- and multi-pinhole SPECT** applications

- Corrections for:
  - Intrinsic PSF
  - Depth of impact
  - Full and simple attenuation
- Three configuration files generate matrix:
  - **Collimator** (pinhole info, wall thickness, etc.)
  - **Detector** (crystal info, projection info, etc.)
  - **Parameters** (matrix size, corrections, etc.)
- Weight matrix imported "**From File**" into STIR

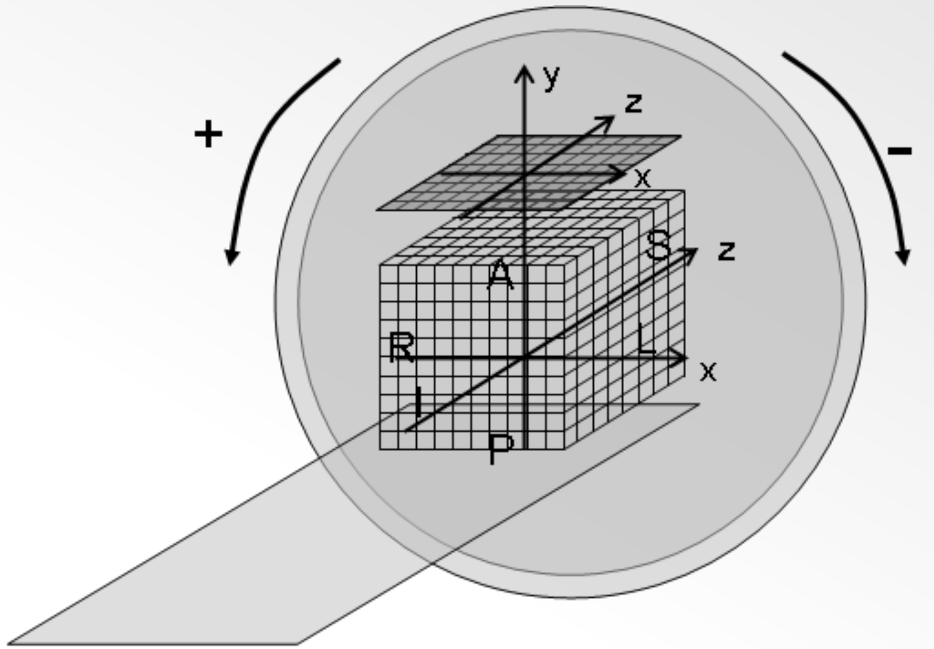

Figure 2. Weight matrix and coordinate system illustration

BIOTIC employs the SPARK™ SPECT scanner

- Developed by Cubresa, Inc. (Winnipeg, Manitoba, Canada)
- Benchtop SPECT scanner utilizing **silicon photomultiplier (SiPM)** technology
- Provides ability to study dynamic and temporal biological processes of disease in small-animal models

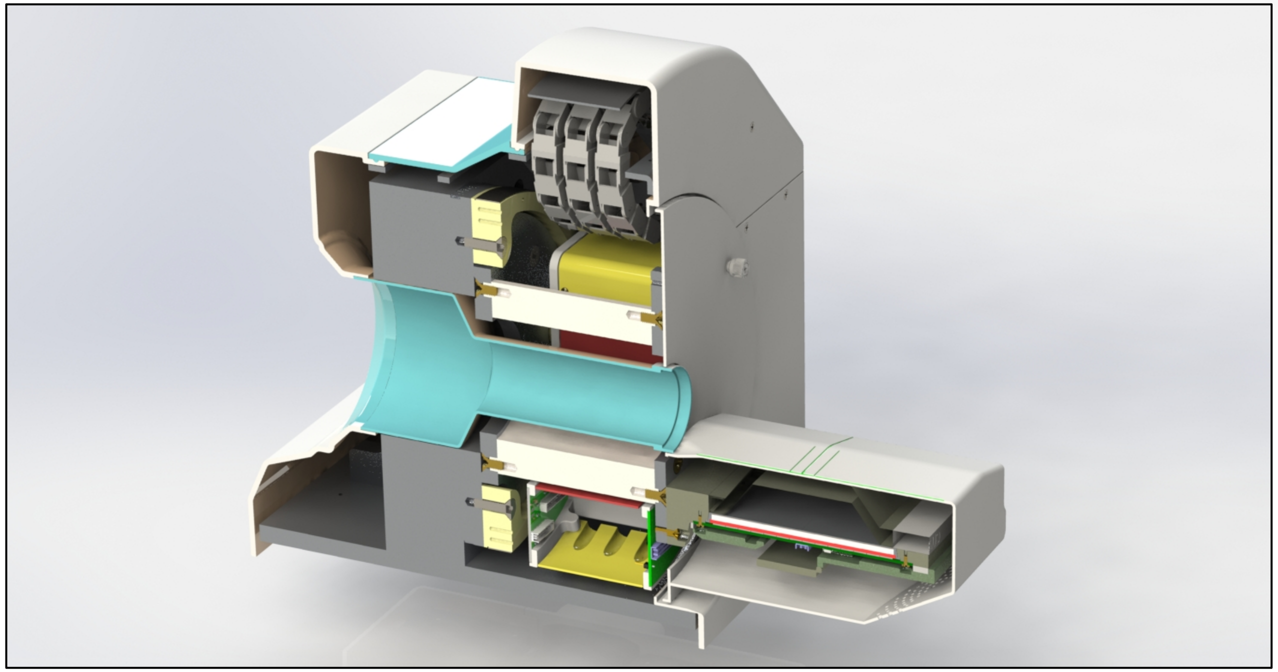

Figure 3. SPARK scanner featuring a CsI(Na) scintillator (102 x 102 x 3 mm^3) coupled to a 14 x 14 SensL C-series SiPM array

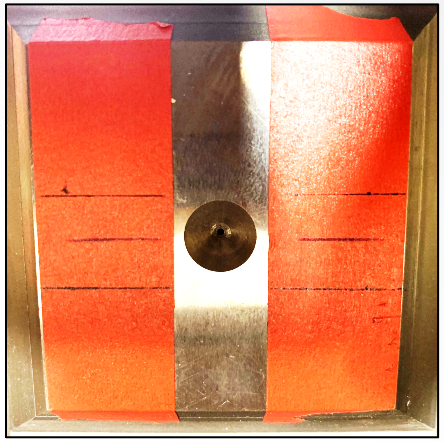

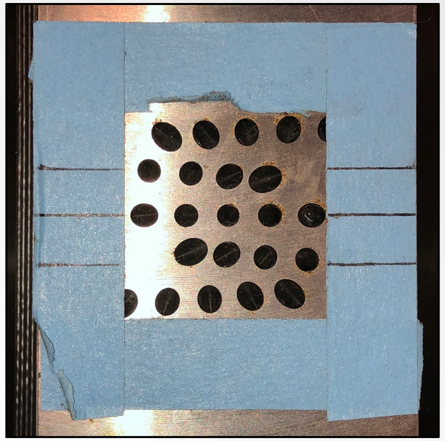

Figure 4. Interchangeable single-pinhole (left) and multi-pinhole (right) tungsten collimators

Understanding the SPARK performance is key to designing studies and developing radiotracers

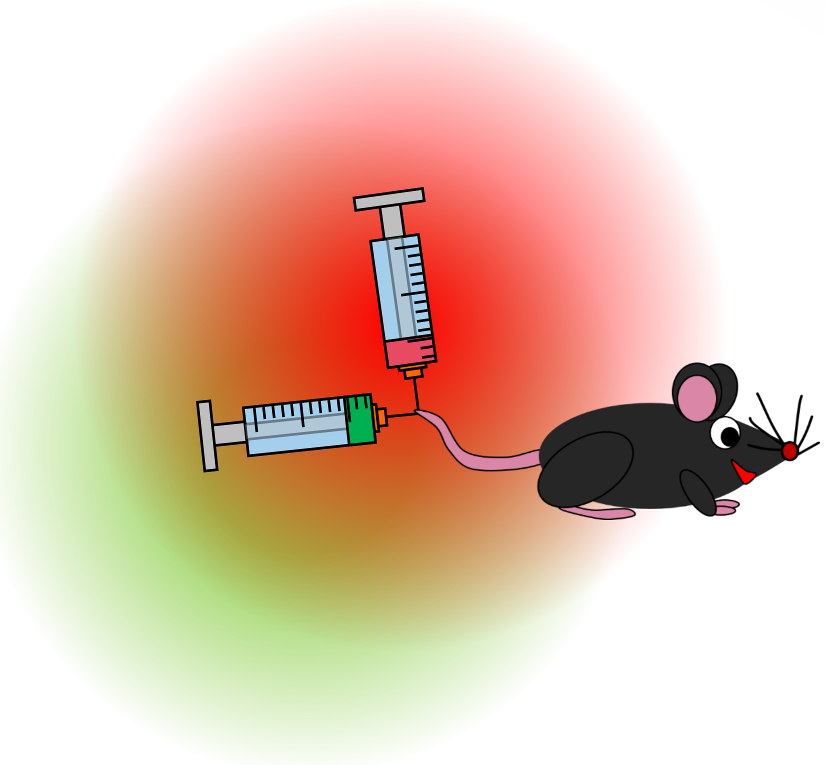

- Interest in **multi-isotope imaging**
  - Reliability of isotope recognition
  - Scatter/cross-talk correction using **triple energy window** (TEW) method
- Monte Carlo is the gold standard for radiation modelling
  - Detailed analysis of TEW with scanner modelled in **GATE v9.0**
- Assess SPARK performance
  - **NEMA NU 1-2018** standard for performance measurements of **γ** cameras
    - Intrinsic, system, and **tomographic measurements** with ^{99m}Tc
    - Validation of Monte Carlo model
  - **TEW feasibility** with ^{111}In and ^{99m}Tc line sources

Pinhole collimators produce high-resolution *tomographic* images, now recon'd with STIR!

Table 1. Tomographic spatial resolution without scatter

Measurement	Experiment	Simulation*	Simulation*
Collimator	Multi-pinhole	Single-pinhole	Single-pinhole
Average FWHM	**1.22 ± 0.16 mm**	**1.53 ± 0.22 mm**	**2.45 ± 0.43 mm**
3 points in air setup: • A ≅ 0.3 MBq/point • t = 40 min • 7.5 mm transaxial and 5 mm axial separation **Reconstructed image:** • 0.25 mm voxels	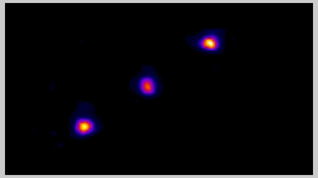	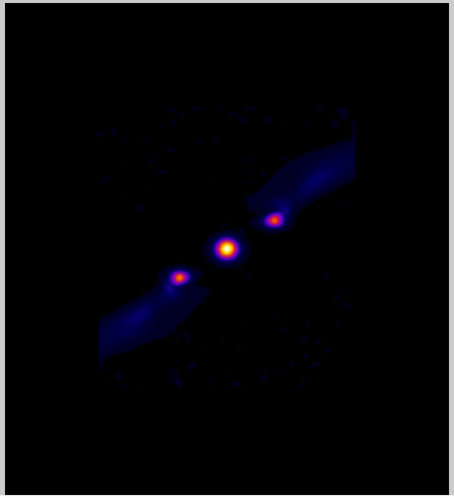	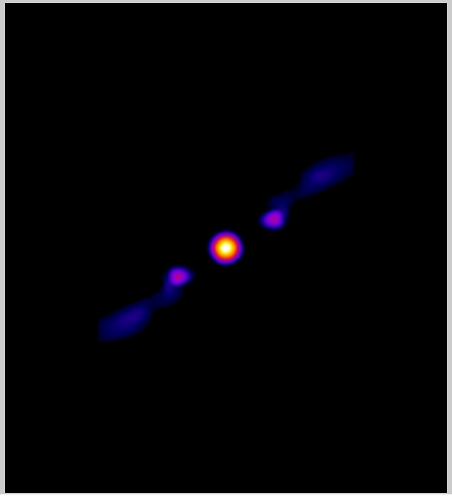
Reconstruction algorithm	OSEM: 4 subsets, 9 subiterations	OSEM: 4 subsets, 9 subiterations	FBP2D
Reconstruction software	Cubresa (default)	**STIR**	**STIR**
Limiting FOV	14 mm axial, 15 mm radial	57.5 mm axial, 23 mm radial	57.5 mm axial, 23 mm radial

- Clinical SPECT: ~10 mm
- Preclinical SPECT: 0.4 – 1.75 mm

*Simulation model validated with NEMA results

DALHOUSIE UNIVERSITY BIOTIC Imaging for Life CUBRESA Molecular Imaging Solutions nova scotia health authority

A simple TEW case with GATE: Two capillary tubes

- **Acquisition parameters:**
  - Projections: 64
  - Duration: 960 s
  - Time/projection: 15 s
  - Activity:
    - ^{99m}Tc: 5 MBq
    - ^{111}In: 5 MBq
    - Diameter: 1.15 mm
    - Separation: 10 mm
- Simulation run-time: 22 h

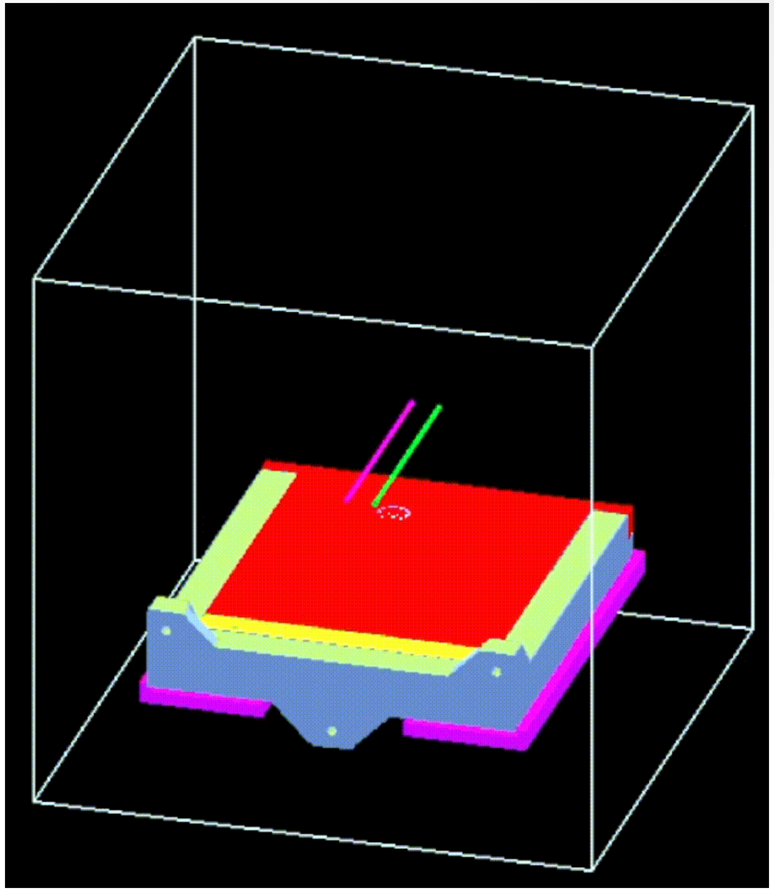

Figure 5. Simulation visualization (^{111}In; ^{99m}Tc)

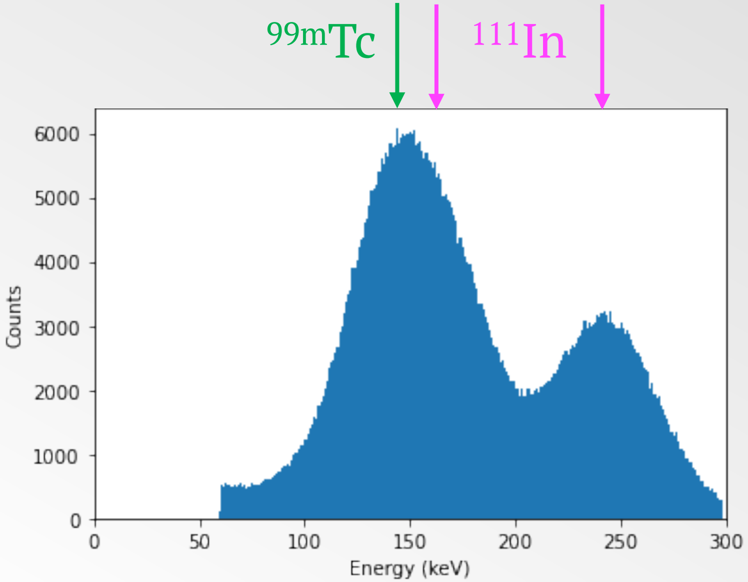

Figure 6. Output energy spectrum with overlapping photopeaks

- ROOT output converted to Cubresa list mode format, processed by TEW, binned for projections, then output to Interfile for STIR recon

Applying the TEW improves image contrast

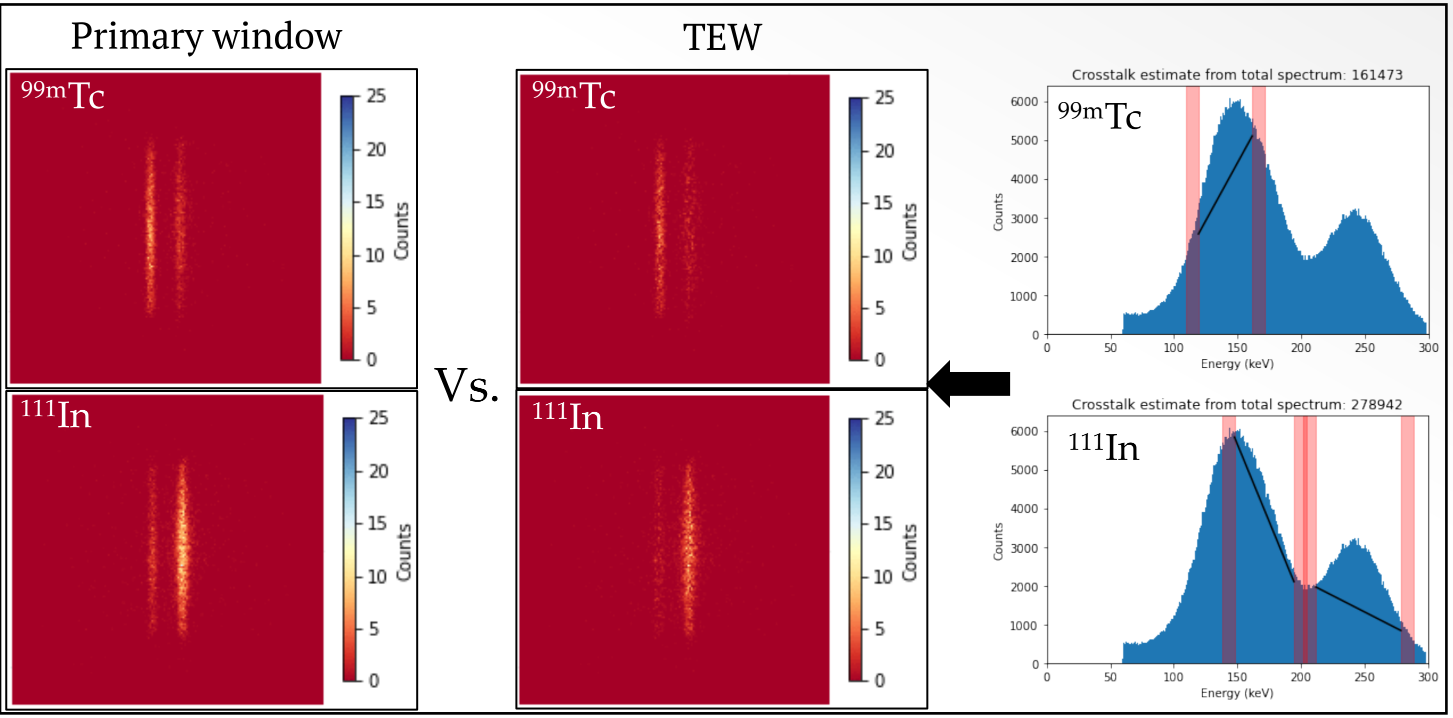

Figure 7. Comparison of projection images obtained from primary energy window (left) and TEW (middle) using the windows illustrated in the energy spectrum (right).

- **Primary window width**: FWTM of photopeak (~28%)
- **Secondary window width**: 10 keV

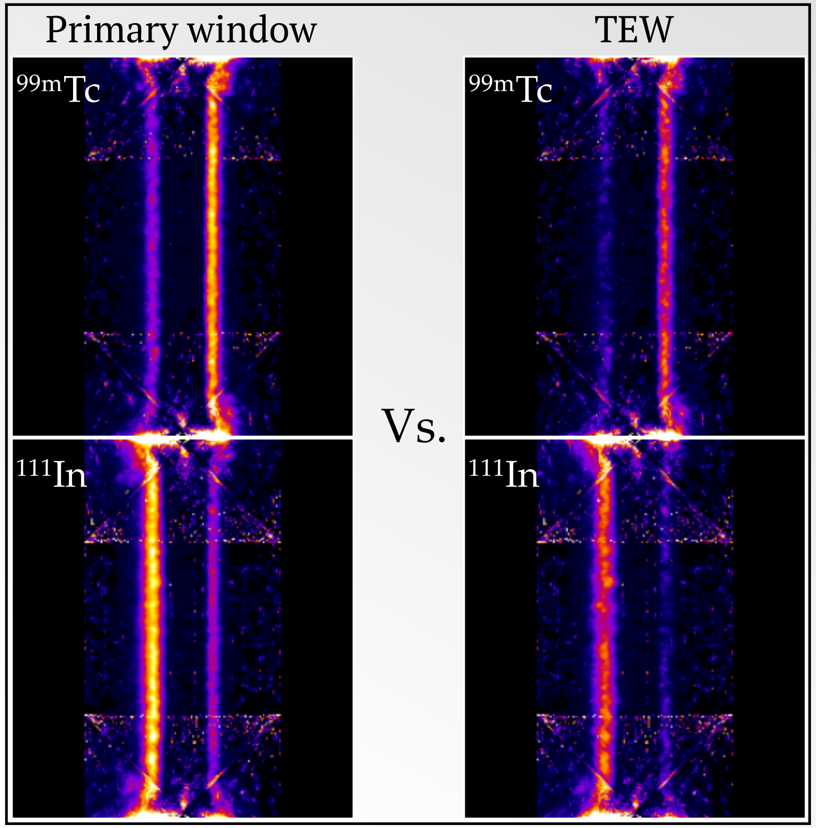

Figure 8. Comparison of reconstructed images from primary energy window (left) and TEW (right). Note that all images are displayed with the same window/level ranging from 0 to 1.

- OSEM: 4 subsets, 16 subiterations

DALHOUSIE UNIVERSITY
BIOTIC Imaging for Life
CUBRESA Molecular Imaging Solutions
nova scotia health authority

Applying the TEW improves image contrast

Table 2. Line source contrast

Energy window	Contrast	CNR
^{99m}Tc	0.33	5.67
^{99m}Tc TEW	**0.46**	**2.13**
^{111}In	0.68	3.64
^{111}In TEW	**0.80**	**2.45**

$$C = \frac{|I_A - I_B|}{I_A + I_B} \qquad CNR = \frac{C}{\sigma^2}$$

TEW improves ^{99m}Tc contrast by 38% and ^{111}In contrast by 18%

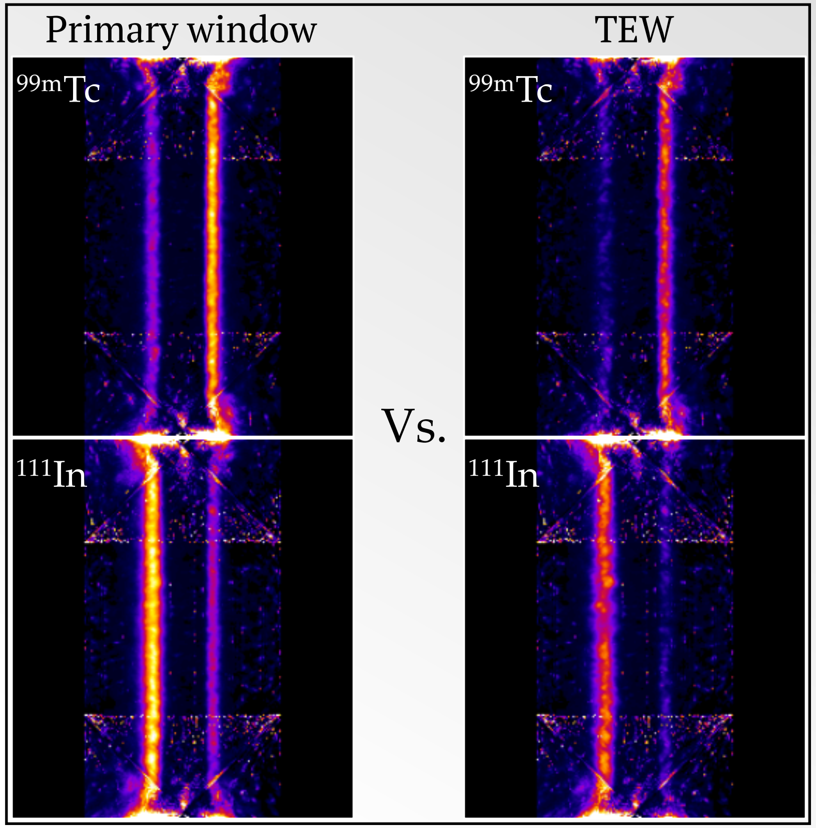

Figure 8. Comparison of reconstructed images from primary energy window (left) and TEW (right). Note that all images are displayed with the same window/level ranging from 0 to 1.

- OSEM: 4 subsets, 16 subiterations

Discussion

- Three points of ^{99m}Tc in air demonstrate comparable resolution for single- and multi-pinhole collimator
  - Multi-pinhole collimator (Cubresa OSEM): 1.22 ± 0.16 mm
  - Single-pinhole collimator (STIR OSEM): 1.53 ± 0.22 mm
- Low intensity artifact extends radially from origin beyond point sources
  - Not apparent in line source images
- Line sources appear straight with uniform activity throughout overlapping FOV
- TEW improves ^{99m}Tc contrast by 38% and ^{111}In contrast by 18%

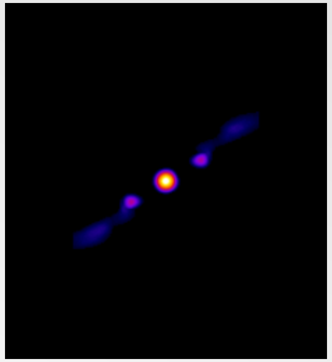

Figure 9. Low intensity artifact

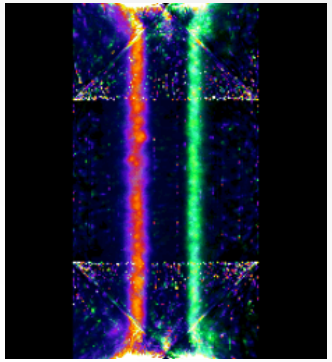

Figure 10. ^{99m}Tc & ^{111}In overlay

Conclusions

- Preliminary results show **pinhole-SPECT image reconstruction is feasible with STIR** using the prototype weight matrix code

- Integrating prototype code into STIR will permit PSF, depth of impact, and attenuation corrections
  - Storing weight matrix from all projections in memory consumes significant RAM
    - Insufficient RAM for corrections
  - STIR calculates weight matrix per projection, significantly reducing RAM consumption

- Integration will expand STIR's publicly available tomographic image reconstruction toolbox, allowing **additional support of complex pinhole-SPECT geometries in a user-friendly format**

References

Fuster, B. M., Falcon, C., Tsoumpas, C., Livieratos, L., Aguiar, P., Cot, A., Ros, D., & Thielemans, K. (2013). Integration of advanced 3D SPECT modeling into the open-source STIR framework: SPECT reconstruction with STIR. *Medical Physics*, *40*(9), 092502. https://doi.org/10.1118/1.4816676

National Electrical Manufacturers Association, NEMA (2019). Standards Publication NU 1-2018: Performance Measurements of Gamma Cameras.

Thielemans, K., Tsoumpas, C., Mustafovic, S., Beisel, T., Aguiar, P., Dikaios, N., & Jacobson, M. W. (2012). STIR: Software for tomographic image reconstruction release 2. *Physics in Medicine and Biology*, *57*(4), 867–883. https://doi.org/10.1088/0031-9155/57/4/867

Clinical SPECT:

Bushberg, J. T. (Ed.). (2012). *The essential physics of medical imaging* (3rd ed.). Wolters Kluwer Health/Lippincott Williams & Wilkins.

Preclinical SPECT:

Austin, D. W., Paulus, M. J., Gleason, S. S., Mintzer, R. A., Siegel, S. B., Figueroa, S. D., Hoffman, T. J., & Wall, J. S. (2006). Design and Performance of a New SPECT Detector for Multimodality Small Animal Imaging Platforms. *2006 IEEE Nuclear Science Symposium Conference Record*, 3008–3011. https://doi.org/10.1109/NSSMIC.2006.356508

Deleye, S., Van Holen, R., Verhaeghe, J., Vandenberghe, S., Stroobants, S., & Staelens, S. (2013). Performance evaluation of small-animal multipinhole μSPECT scanners for mouse imaging. *European Journal of Nuclear Medicine and Molecular Imaging*, *40*(5), 744–758. https://doi.org/10.1007/s00259-012-2326-2

Magota, K., Kubo, N., Kuge, Y., Nishijima, K., Zhao, S., & Tamaki, N. (2011). Performance characterization of the Inveon preclinical small-animal PET/SPECT/CT system for multimodality imaging. *European Journal of Nuclear Medicine and Molecular Imaging*, *38*(4), 742–752. https://doi.org/10.1007/s00259-010-1683-y

McElroy, D. P., MacDonald, L. R., Beekman, F. J., Yuchuan Wang, Patt, B. E., Iwanczyk, J. S., Tsui, B. M. W., & Hoffman, E. J. (2002). Performance evaluation of A-SPECT: A high resolution desktop pinhole SPECT system for imaging small animals. *IEEE Transactions on Nuclear Science*, *49*(5), 2139–2147. https://doi.org/10.1109/TNS.2002.803801

van der Have, F., Vastenhouw, B., Ramakers, R. M., Branderhorst, W., Krah, J. O., Ji, C., Staelens, S. G., & Beekman, F. J. (2009). U-SPECT-II: An Ultra-High-Resolution Device for Molecular Small-Animal Imaging. *Journal of Nuclear Medicine*, *50*(4), 599–605. https://doi.org/10.2967/jnumed.108.056606

Acknowledgements

Dr. Kim Brewer

Dr. Steven Beyea

Dr. Kris Thielemans

Dr. Daniel Deidda

Bob Schellenberg

Ryan Sparkes

Cubresa, Inc.

Nova Scotia Graduate Scholarship Program

Thank you!

Matthew Strugari

matthew.strugari@dal.ca

Dec. 3, 2020